https://doi.org/10.15302/frontphys.2026.022200

RESEARCH ARTICLE

Hyperbolic absolute instruments

Tao Hou[1,2], Huanyang Chen[1,2,†]

[1]Department of Physics, Xiamen University, Xiamen 361005, China

[2]Department of Physics, Xiamen University Malaysia, Sepang 43900, Malaysia

Corresponding author. E-mail: [†]kenyon@xmu.edu.cn

Received March 24, 2025; Accepted May 30, 2025

Supporting Information

Note S1: The calculation of integral in Eq. (9)

In order to solve the integral equation of Abel's type in Eq. (9), we divide $\Delta\varphi(L)$ by $\gamma\sqrt{L^2-L'^2}$, where L' is an integration parameter, and integrate with respect to L' from L_0 to L:

$$\begin{aligned}\int_{L_0}^{L}\frac{\Delta\varphi(L')dL'}{\gamma\sqrt{L^2-L'^2}}&=\int_{L_0}^{L}\int_{\tau_-(L')}^{\tau_+(L')}\frac{d\tau}{\sqrt{L'^2-N(\tau)^2}}\frac{L'dL'}{\sqrt{L^2-L'^2}}\\&=\int_{\tau_-(L)}^{\tau_+(L)}\int_{N(\tau)}^{L}\frac{L'dL'}{\sqrt{L^2-L'^2}}\frac{d\tau}{\sqrt{L'^2-N(\tau)^2}}\\&=\int_{\tau_-(L)}^{\tau_+(L)}\left[-\arcsin\sqrt{\frac{L^2-L'^2}{L^2-N(\tau)^2}}\right]_{L'=N(\tau)}^{L'=L}d\tau\\&=\int_{\tau_-}^{\tau_+}(0-(-\frac{\pi}{2}))d\tau=\frac{\pi}{2}(\tau_+-\tau_-)\end{aligned}, \tag{S1}$$

where we have inverted the order of integration and adjusted the integration limits appropriately (see Fig. S1) [28]. Here, we set $\Delta\varphi=\pi/m'=\gamma\pi/m$, where m' is set as a rational number to satisfy the closed ray in HAI. Then we can obtain from Eq. (S1):

$$\mathrm{In}\frac{r_+}{r_-}=\frac{2}{m}\arccos(L_0/L)\,. \tag{S2}$$

Here we define a function $f(r)$, and it satisfy the conditions $f(r_-)=r_+$ and $f(r_+)=r_-$ for arbitrary turning points $r_\pm$. i.e.

$$r_\pm=f(r_\mp)\,. \tag{S3}$$

Then we obtain $f(f(r))=r$. This implies that the graph of $f(r)$ is symmetric with respect to the axis $f(r)=r$ and intersects at the point $r=r_m$ when satisfying the condition $r_+=r_-$. Notably, the intersection corresponds to the case $L=L_0$ (the lowest point of the graph in Fig. 4(b)), i.e., circular ray trajectory. With the function $f(r)$ defined this way, we can express r_- in terms of $f(r_+)$ or vice versa. Taking the fact that $L=N=nr$ at $r=r_\pm$ and omitting the index of $r_\pm$, we obtain the general index as

$$n(r)=\frac{L_0}{r\cos(\frac{m}{2}\mathrm{In}(f(r)/r))}\,. \tag{S4}$$

Note S2: Other examples of hyperbolic absolute instruments

Hyperbolic Luneburg lens (HLL) profile

As a well-known AI, Luneburg lens (LL) profile ($n=\sqrt{(2-r^2)}$) focuses all the rays from the object r_A to the image with the same radius $r_B=r_A$, and the corresponding ray trajectories form ellipses centered at the origin [S1] (see Fig. S2(a)). Here, we adopt the same $f(r)=\sqrt{(2-r^2)}$ and m=2 as LL for the case of γ=1. The ray and wave in HLL still retain the focusing characteristic of LL profile even though the refractive index distribution is completely different (see Fig. 1(d) and Fig. S2(b,c)). While both Luneburg lens profile and HLL profile have similar outer boundary, parts of rays can bypass the former but diverge to the latter.

It is worth noting that there is interference in areas other than the vicinity of the focal point due to the convergence of multiple rays during propagation.

Hyperbolic Eaton/Miñano lens (HEL) profile

Traditional Eaton/Miñano lens (EL) profile ($n=\sqrt{(2/r-1)}$) corresponds to elliptic motion in the Newton potential in mechanics, where ray trajectories are confocal ellipses with focus at the origin and with the main semiaxes of unit length (see Fig. S2(d)) [S1]. Here we adopt the same $f(r)$=2-r and m=1 for the case of γ=1, the ray and wave maintain self-focusing properties at the objects after rotating around the center (see Figs. S2(e,f)). Similar to HLL, interference effects arise due to the convergence of multiple rays during propagation.

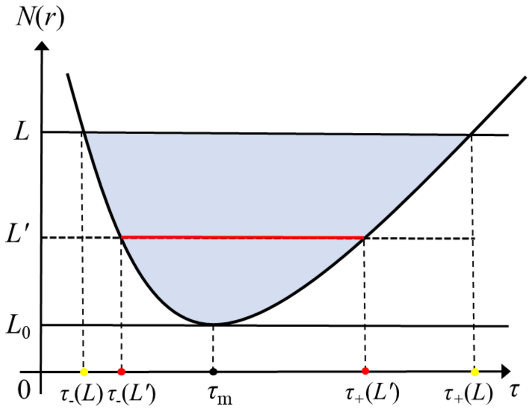

Fig. S1 The change of integration limits in Eq. (S1) illustrating that $\int_{L_0}^{L}\int_{\tau_-(L')}^{\tau_+(L')}\frac{d\tau}{\sqrt{L'^2-N(\tau)^2}}\frac{L'dL'}{\sqrt{L^2-L'^2}}=\int_{\tau_-(L)}^{\tau_+(L)}\int_{N(\tau)}^{L}\frac{L'dL'}{\sqrt{L^2-L'^2}}\frac{d\tau}{\sqrt{L'^2-N(\tau)^2}}$.

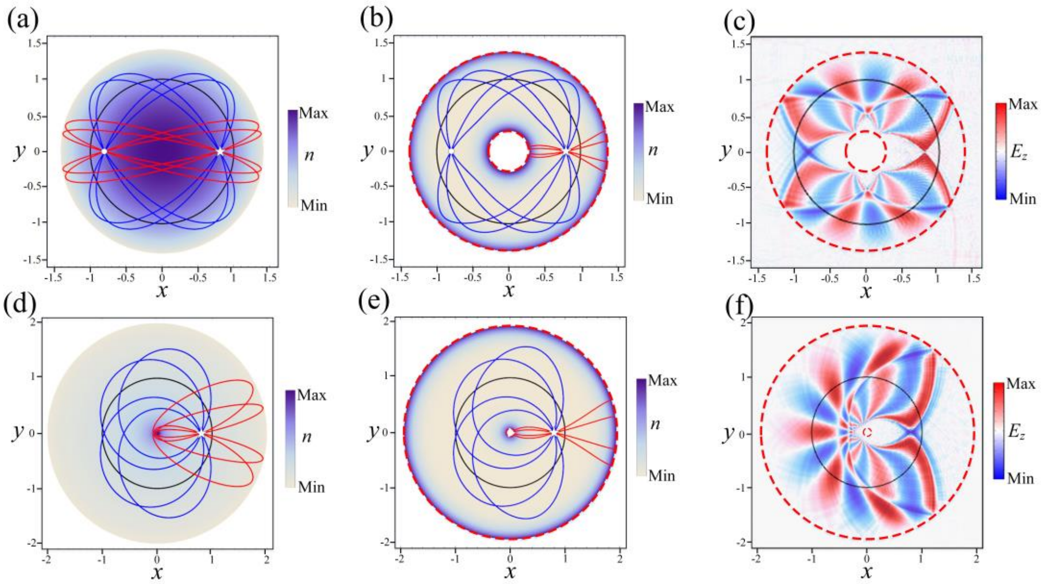

Fig. S2 The rays and electric field E_z in the **(a)** LL profile, **(b,c)** HLL profile, **(d)** EL profile and **(e,f)** HEL profile. The white stars and circles represent the incident points (r_0, φ_0) = (0.8, 0) and the images, respectively. The red and blue rays represent the rays with incident direction $\left|\frac{dr}{rd\varphi}\right|_{initial}>1$ and $\left|\frac{dr}{rd\varphi}\right|_{initial}<1$, respectively. The black solid boundaries and red dotted boundaries represent the condition n=1 and n=∞, respectively.

Reference

[S1] U. Leonhardt and T. Philbin, Geometry and Light: The Science of Invisibility, New York: Dover, 2010